PERGAMON

International Journal of Heat and Mass Transfer 43 (2000) 935–943

International Journal of HEAT and MASS TRANSFER

www.elsevier.com/locate/ijhmt

Ray effect mitigation in jet fire radiation modelling

P.S. Cumber*

BG Technology, Gas Research and Technology Centre, Loughborough LE11 3GR, UK

Received 15 May 1998; received in revised form 21 May 1999

Abstract

The radiation fields of jet fires are highly anisotropic, exhibiting a significant ray effect, making their calculation potentially a computationally intensive process. Two quadrature strategies for evaluating the incident radiative flux distribution are presented and analysed, both strategies are shown to be highly efficient. As well as mitigating the ray effect by improvements in computational efficiency, false convergence is avoided as numerical error estimates and bounds are derived and demonstrated to be sharp. © 2000 BG Technology. Published by Elsevier Science Ltd. All rights reserved.

Keywords: Ray effect; Adaptive quadrature; Discrete transfer method

1. Introduction

The accurate modelling of thermal radiation is important in many combusting systems. The calculation of the external radiation field of free jet flames is the subject of the present article. The generic nature of free jet flames makes their study and advances in their computation a benefit to a range of application areas, being directly relevant for example to efficient and environmentally friendly furnace design and the safety assessment of flaring and venting of flammable gases. Considering flaring and venting operations further, it is necessary to predict the incident radiative flux to the surrounding area from a flare or the jet fire that might be established should the dispersing gas ignite accidentally. The specific problem of interest is the efficient calculation of radiative heat transfer and numerical error estimation. The radiative flux incident to a point s on a surface or a radiometer can be expressed by the integral,

$$q_- = \int_{\Delta\Omega}\int_0^\infty I_\lambda(\Omega, s)\cos\theta \, \mathrm{d}\lambda \, \mathrm{d}\Omega \tag{1}$$

where I_λ is the spectral intensity, λ denotes wavelength, θ is the angle of incidence and $\Delta\Omega$ is the field of view of the receiver. The spectral intensity distribution can be calculated, for example, by an exponential wide-band model [1], alternatively the spectral integration is avoided and the total intensity is calculated using a more empirical approach, such as a mixed-grey-gas model [2].

For any mathematical model, to have confidence in the predicted flow and heat transfer fields, some estimate or bound on the prediction error is required. One numerical artefact that can seriously hamper the rigorous calculation of radiative heat transfer is the ray effect. The ray effect occurs when the continuous incident intensity distribution is approximated by a discrete angular quadrature in the numerical evaluation

* Tel.: +44 1509 282429; fax: +44 1509 283119.
E-mail address: peter.cumber@bgtech.co.uk (P.S. Cumber).

PII: S0017-9310(99)00172-6

Nomenclature

E_{bound}	error bound
E_{est}	error estimate
G_1, P_2, P_i	labels for ray orientations
I	total intensity
I_λ	spectral intensity
N_{bad}	radius of refinement
N_θ, N_φ	number of rays in the θ and φ co-ordinate directions
q_-	incident flux
r	radial co-ordinate direction
z	axial co-ordinate direction
s	point vector
β	correction factor in error bound, see Eq. (8)
$\Delta\theta, \Delta\varphi$	ray spacing in the θ and φ co-ordinate directions
$\Delta\Omega$	field of view
ε_{tol}	tolerance for adaption criteria
Ω	orientation vector
θ	angle of incidence
λ	wavelength
φ	angle of rotation

Subscripts

c	quantity associated with hemispherical element
co	coarse ray mesh quantity
fi	fine ray mesh quantity
extrap	extrapolated quantity

Superscript

c	quantity associated with hemispherical element

of the incident flux integral. If the discrete angular quadrature set is insufficient to accurately represent the continuous distribution then physically unrealistic incident flux distributions can be predicted, with local maxima and minima, where the opposite would intuitively be expected. When the ray effect is significant, radiative flux predictions with small numerical error are often computationally expensive to calculate, requiring a detailed prediction of the incident intensity distribution. Further discussion of the ray effect, and its mitigation can be found in [3], and the references therein. A common thread through the papers cited in [3], is the ray effect mitigation strategies presented are demonstrated using idealised computationally challenging test problems, but evaluating how important the ray effect might be for more realistic situations is difficult to appreciate. In this article efficient quadrature strategies over solid angle are presented, analysed and their ability to mitigate the ray effect in natural gas jet fires is evaluated.

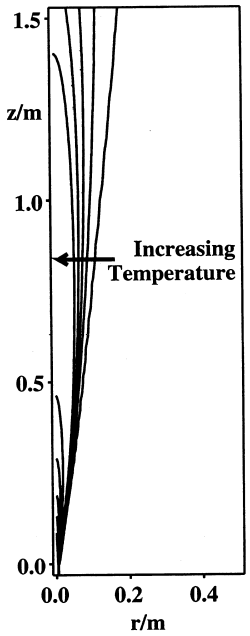

Fig. 1. Predicted temperature field for the laboratory scale fire ($Re = 8800$), contour values of 300, 600, 900, 1200 and 1500 K.

The calculation of the external radiation field of a jet fire is a particularly challenging task, as the intensity field is highly anisotropic with a relatively small hot volume of gas dominating the heat transfer external to the flame envelope. We shall consider the prediction of the incident external flux using the discrete transfer method [4]. By way of illustration, the calculation of the external radiation field of a laboratory scale jet fire and a field scale sonic natural gas jet fire are used as test problems, to prove the ideas and developments discussed below.

2. Flame structure model

The laboratory scale jet fire considered is a rim-stabilised axisymmetric methane flame. The flame has a Reynolds number of 8800 based on the bulk velocity at the nozzle exit. The nozzle has a diameter of 8.4

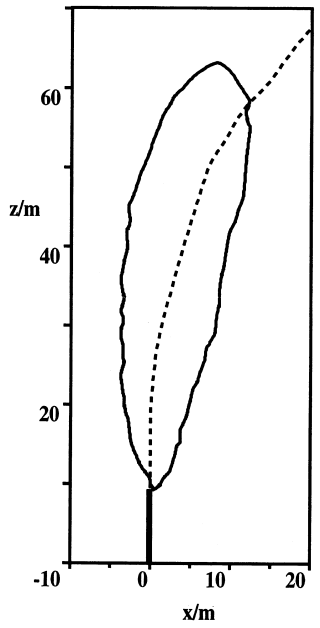

Fig. 2. Measured flame envelope and the predicted jet trajectory viewed from a crosswind direction.

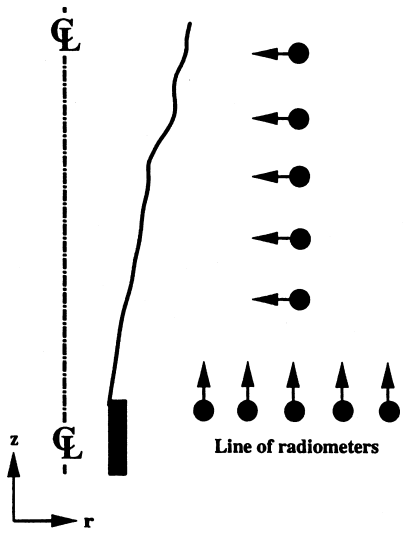

Fig. 3. A schematic diagram of the laboratory scale jet flame and the two lines of radiometers.

mm. More details of the experiment can be found in [5]. Fig. 1 shows a prediction of the mean temperature field, contours of 300, 600, 900, 1200 and 1500 K are shown. This flow is computationally inexpensive to calculate, and turbulence–radiation interaction effects have been found to be small [6], making it possible to use a mean temperature analysis to model the external radiation field.

The modelling of the radiation flux requires some representation of the flame structure, which is predicted using a model based on the boundary layer equations [7]. The model consists of a system of parabolic equations formulated in terms of Favre averaged quantities, to reflect the variable density character of the flow. The system of equations is closed using the k–ε turbulence model [8]. Turbulent combustion is modelled using a conserved scalar/prescribed probability density function (pdf) approach combined with a laminar flamelet library with a radiative heat loss of 15% [9]. The prescribed pdf is a β-function, which requires two additional transport equations for the mean mixture fraction and its variance. The system of transport equations, together with the source prescription and air entraining boundary conditions in the radial direction, are solved using a finite volume marching scheme, marching in the downstream direction [7]. A detailed description of the model can be found in [1] and the references cited therein.

The sonic natural gas jet fire considered below has a pressure ratio of 1.68 issuing from a stack with a diameter of 385 mm into an atmospheric boundary layer with a wind speed of 6.2 m/s measured at a height of 10 m. The full details of the field scale test and the reacting flow simulation can be found in [10]. Fig. 2 shows the observed flame envelope and the predicted jet trajectory, viewed from the cross-wind direction.

3. Radiation modelling

To evaluate the incident flux integral it is expressed in spherical co-ordinates and the field of view discretised with a uniform spacing in the angle of rotation (φ) and angle of incidence (θ). For the remainder of this article such a distribution of rays will be described as 'uniform'. The incident intensity distribution is assumed piece-wise constant over the field of view of the receiver, with each element of the discretisation taking the value of the incident intensity at its centroid as being representative of the whole element. The incident intensity over an element is calculated by tracing the ray with orientation defined by the centroid, through the computational domain, noting the control volumes of the finite volume grid traversed, length of ray segment, and local thermo-chemical quantities. The ray trace is terminated at the computational boundary. The stored data is then used as an input to a model for participating media which solves the equation of radiative heat transfer. The incident flux is approximated as,

$$q_- = \sum_c I(\varphi_c, \theta_c)\frac{1}{2}\sin 2\theta_c \sin\Delta\theta\,\Delta\varphi \qquad (2)$$

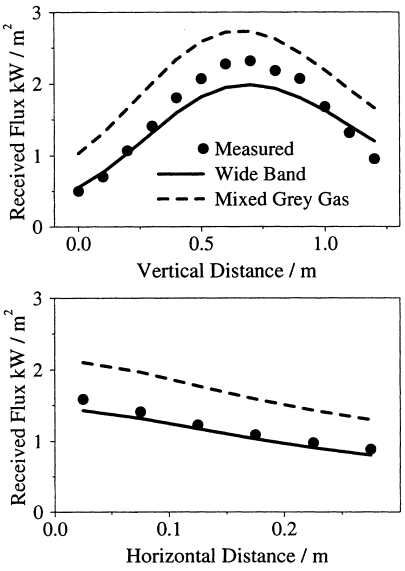

Fig. 4. Incident flux distributions from a laboratory scale jet fire ($Re = 8800$, diameter $= 8.4$ mm) using 3072 rays for (a) vertical line ($r = 0.4$ m) and (b) horizontal line of receivers ($z = 0$).

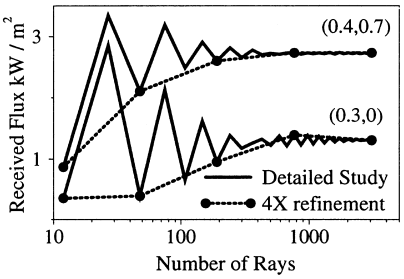

Fig. 5. Convergence history of incident flux predictions at the receivers (0.4, 0.7) and (0.3, 0) using a uniform ray distribution, $(N_\varphi, N_\theta) = (3I, I)$, $I = 2, 3, \ldots, 32$.

where the $\sum$ is over the field of view of the receiver and (φ_c, θ_c) denotes spherical co-ordinates on the unit hemisphere. For clarity the λ subscript has been dropped and I denotes the total intensity.

This is not the only quadrature rule formulated in terms of spherical co-ordinates, for example [11] derived more accurate quadrature rules analogous to the Newton Cotes trapezoidal rule and a Gaussian quadrature rule. These quadrature rules will not be considered further here as they cannot easily be combined with the techniques discussed below.

To aid appreciation of the configuration of the radiometers with respect to the flame Fig. 3 is a schematic of the laboratory scale jet fire showing the location and orientation of the radiometers. Fig. 4 shows predictions of received radiative flux and the measured received flux distribution, for a vertical and horizontal line of radiometers about the laboratory scale flame. Locating the origin of the axisymmetric co-ordinate system (r, z), at the centre of the nozzle exit plane, see Fig. 1, the vertical line of 13 receivers were located between (0.4, 0) and (0.4, 1.2) with a uniform spacing in the axial co-ordinate direction. The horizontal line of six uniformly spaced receivers were located between (0.05, 0) and (0.3, 0). The field of view of the radiometers is 150° with a spectral window of 1–6 μm. For each line of radiometers two predictions are shown. The full line was calculated using an exponential wide-band model [1]. This model calculates a representation of the spectral intensity distribution, accounting for the spectral window of the receivers. Good agreement between the model prediction and the measurements is achieved, the largest discrepancy occurring at the measured incident flux peak in the vertical line of receivers. The second prediction denoted by the dashed line is a prediction of incident flux using a mixed-grey-gas model [2]. This is a computationally frugal model based on a curve fit to total emissivity data and, therefore, cannot account for the limited spectral window, hence it overpredicts the observed flux distribution, although the predicted flux qualitatively agrees with the measurements. Unless stated otherwise, the predictions of incident flux discussed below were calculated using the mixed grey gas model. This is acceptable as we are interested in evaluating techniques for accelerating convergence of the angular quadrature which should be insensitive to the model adopted for the participating media provided it is physically plausible.

The predictions in Fig. 4 are ray independent to the level of resolution of the figure. This was verified by predicting the incident flux distributions with three rays initially and successively doubling the number of rays in each spherical co-ordinate direction until the solution remained unchanged. The received flux distribution for the 3072 ray prediction differed from the 768 ray prediction by over 6%. A predicted incident flux distribution calculated with 12,288 rays, verified that the 3072 ray prediction, shown in Fig. 4, has a numerical error of less than 0.5%. This is one approach for assessing the sensitivity of numerically predicted fields to the number of rays used. Although insight is gained into the magnitude of the numerical error, it is a computationally expensive procedure. The field of view is a two-dimensional manifold, therefore, every refinement requires of the order of four times as much computer run-time than the previous ray distribution to calculate. Doubling the number of rays in each spherical co-ordinate direction, rather than a less substantial refinement, is necessary as no error estimate or error bound is available. A measure of the numerical error is the relative difference in two successive predic-

tions of incident flux in the ray convergence sequence, but this is not always a good indication of the true error. The only link between relative difference and numerical error is that they both asymptote to zero as the number of rays is increased.

Discussing the ray convergence issue further, it is worthwhile to focus attention on two representative radiometers oriented vertically and horizontally located at $(r, z) = (0.4, 0.7)$ and $(0.3, 0)$, respectively. In Fig. 5 the full convergence history is shown for the two radiometers. The predicted incident flux as a function of the number of rays is plotted for the ray distributions, $(N_\varphi, N_\theta) = (3I, I)$, $I = 2, 3, \ldots, 32$. The incident flux predictions calculated by doubling the number of rays in each spherical co-ordinate direction are also indicated (labelled 4X refinement in Fig. 5). Increasing the number of rays by four times at every refinement does not give an accurate record of the convergence history, neglecting the wealth of structure present. For most applications the convergence history is of little importance other than to confirm ray independence, although as we shall discuss below the fine structure does prevent the successful application of extrapolation techniques for error evaluation. Considering the detailed ray convergence histories, convergence behaviour for both receivers is poor, the rate of convergence being much slower than the order of the quadrature rule, based on a Taylor series analysis would indicate. This is a manifestation of the ray effect and would be present to some degree in any radiation model where the continuous incident intensity distribution was approximated by a discrete angular quadrature.

For jet fires the ray effect has serious consequences for predicting the external radiation field, as slow convergence implies large computational cost. The oscillatory behaviour also makes it likely that false convergence may be inferred from a refinement study where the number of rays used at each refinement is not sufficient. One final difficulty is the oscillatory behaviour prevents the application of error estimation techniques such as Richardson extrapolation, as the regularity assumption is violated [12].

4. Ray effect mitigation strategies

4.1. Staggered ray distributions

The oscillatory behaviour in the ray convergence histories is due to sensitivity of the predicted incident flux to changes in the ray distribution in the φ co-ordinate direction. From the analysis of the detailed convergence histories shown in Fig. 5, a ray distribution 'staggered' in the φ co-ordinate direction,

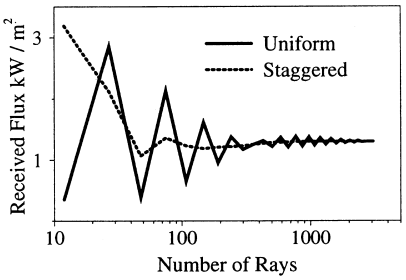

Fig. 6. Convergence history of incident flux predictions at the receiver (0.3, 0) using a uniform and staggered ray distribution, $(N_\varphi, N_\theta) = (3I, I)$, $I = 2, 3, \ldots, 32$.

$$\begin{aligned}&(\varphi_i, \theta_j) = \big(i\Delta\varphi, (j-0.5)\Delta\theta\big), \quad j \text{ even}\\ &(\varphi_i, \theta_j) = \big((i-0.5)\Delta\varphi, \quad (j-0.5)\Delta\theta\big), \quad j \text{ odd}\\ &i = 1, 2, \ldots, N_\varphi, j = 1, 2, \ldots, N_\theta\end{aligned} \tag{3}$$

is suggested as a possible improvement over a uniform ray distribution. This simple modification radically changes the convergence behaviour as exhibited in Fig. 6, which shows the convergence history for a staggered and uniform ray distribution for the receiver located at (0.3, 0). In Fig. 6 the predicted incident flux as a function of the number of rays is plotted for the ray distributions $(N_\varphi, N_\theta) = (3I, I)$, $I = 2, 3, \ldots, 32$. The oscillatory behaviour of the uniform ray distribution is damped and convergence is accelerated. This is an adhoc rule with limited theoretical basis that is simple to implement, but for every radiometer location the improved convergence behaviour is profound.

This simple modification improves convergence behaviour, but an expensive ray refinement study is still required to confirm that the predictions of incident flux are ray independent. Some estimate or measure of the numerical error other than the relative difference is required. The improved convergence behaviour achieved using staggered ray meshes implies Richardson extrapolation is likely to be valid. The extrapolation formula, for the quadrature rule (2), over a single element of the hemispherical mesh can be written,

$$\begin{aligned}&q^c_{-,\text{extrap}} = q^c_{-,\text{fi}}\frac{1}{1-\gamma} - q^c_{-,\text{co}}\frac{\gamma}{1-\gamma} + O\big(\Delta\theta^a\,\Delta\varphi^b\big),\\ &\gamma = 0.25,\ a+b=3\end{aligned} \tag{4}$$

This is derived by taking a linear combination of a coarse ($q^c_{-,\text{co}}$, 1 ray) and fine ($q^c_{-,\text{fi}}$, 4 ray) distribution such that the leading term in the truncation error is eliminated, giving a higher order prediction. Taking $q^c_{-,\text{extrap}}$ to be close to the ray converged incident flux, an error estimate can be derived,

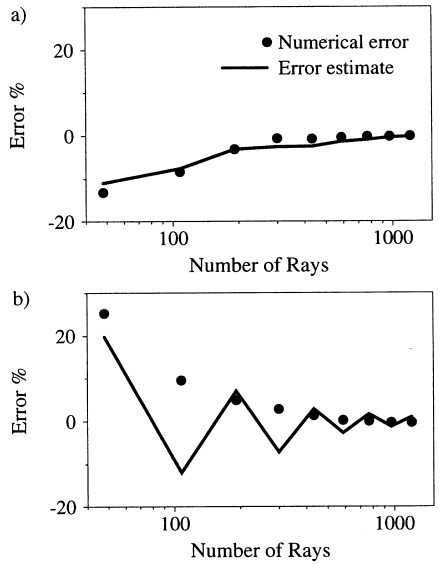

Fig. 7. Actual and estimated error for the receiver (0.4, 0.7) for a (a) staggered ray distribution and (b) uniform ray distribution $(N_\varphi, N_\theta)=(3I, I)$, $I = 2, 3, \ldots, 32$.

$$E^c_{\text{est}} = q^c_{-,\text{extrap}} - q^c_{-,\text{fi}} \tag{5}$$

The above analysis can be applied directly to the whole field of view as the extrapolation formula is linear. Fig. 7 shows the numerical error as a function of number of rays and the extrapolated error estimate using a staggered and uniform ray distribution for the receiver (0.4, 0.7). The points labelled 'numerical error' are the difference between the prediction and an accurate prediction calculated with 12,288 rays, estimated to be within 0.5% of the ray converged value. The uniform ray mesh error estimate poorly reflects the true numerical error, unable to predict its sign. The staggered ray mesh error estimate is acceptable, correctly predicting the convergence behaviour. The performance of the extrapolated error estimate for the staggered and uniform ray distributions shown in Fig. 7 is typical of all the receiver locations and orientations.

4.2. Adaptive quadrature

The improved performance of the staggered ray distribution for jet fire radiative flux modelling compared to the uniform ray distribution is achieved by reducing the sensitivity of the incident flux prediction to variations in the ray distribution in the φ co-ordinate direction. However, this quadrature strategy only partially mitigates the ray effect for receivers remote from the strongly emitting portion of the jet fire. In such situations an adaptive quadrature strategy should be more efficient.

An adaptive quadrature algorithm can be divided into three components; a quadrature rule, an initial coarse ray distribution and an adaption criterion. The quadrature rule used is the piece-wise constant quadrature formula, applied on an element by element basis. The adaption criterion used is the extrapolated error estimate (5) exceeds some user defined tolerance,

$$\frac{|E^c_{\text{extrap}}|}{q^c_{-\text{fi}}} > \varepsilon_{\text{tol}} \Longrightarrow \text{Refine element} \tag{6}$$

A limited numerical study revealed the predicted incident flux is relatively insensitive to the adaption tolerance provided it is sufficiently small, i.e. of the order of 0.1. This is not surprising as there is no bias in the error distribution on the hemisphere and a degree of error cancelation in the numerical integration of the incident flux integral is likely. In addition a secondary adaption criteria was implemented such that an adapted elements neighbouring elements up to a radius of N_{bad} are also refined,

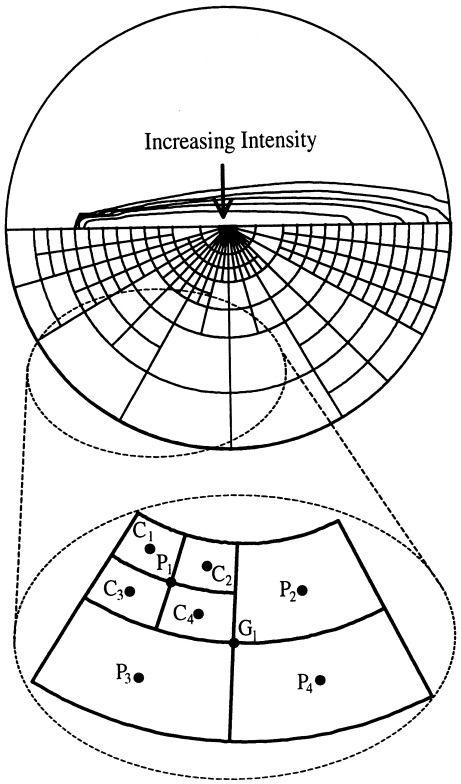

Fig. 8. Contour plot of half of a symmetric incident intensity distribution for the receiver (0.4, 0.7) projected onto a plane, with equi-logaqrithmically spaced contours, (contour values, 0.22, 0.46, 1, 2.2, and 4.6 W m^{-2} sr^{-1} and an adapted ray distribution with an enlargement of a portion of an adapted ray distribution.

$$(\varphi_c, \theta_c) = (\varphi_i, \theta_j) \text{ is refined} \Longrightarrow (\varphi_{i\pm\alpha}, \theta_{j\pm\beta}) \quad \text{are refined,} \quad \alpha+\beta \le N_{\text{bad}} \tag{7}$$

For the jet fire, $Re = 8800$, only three rays $(N_\varphi, N_\theta) = (3,1)$ in the initial ray distribution with N_{bad} set to one are required to ensure the adaptive quadrature process converges to the ray independent incident flux as more levels of refinement are introduced.

The application of adaptive quadrature to the incident flux evaluation is exhibited in Fig. 8, which shows half the incident intensity distribution for the receiver $(r, z) = (0.4, 0.7)$, projected onto a two-dimensional plane, with an adaptive ray distribution, taking advantage of the line of symmetry in the incident intensity distribution. Five equi-logarithmically spaced contours are shown (contour values 0.22, 0.46, 1, 2.2 and 4.6 kW m^{-2} sr^{-1}). The incident intensity distribution is significant over a small portion of the field of view, which is reflected in the pattern of adaption. For the ray distribution shown in Fig. 8, four levels of refinement were prescribed, with the first two coarsest levels being non-adaptive. In all 396 rays were used to evaluate the incident flux, with an error of less than 1%. If no adaption were used 768 rays would be required to give a uniform distribution at the finest level of refinement in the adaptive quadrature strategy.

The adaptive quadrature strategy can be combined with the extrapolated error estimate as fine ray mesh is generated automatically as necessary to make the regularity assumption required to formulate the extrapolated error estimate valid. However, we choose to derive an error bound rather than error estimate as this is also a useful property for determining ray independence. An error bound can be derived from the extrapolated error estimate (5) by taking the summation of the absolute value of the error estimate applied on an element by element basis. A sharper error bound can be derived by including a correction for the partially adapted elements similar to that indicated by the portion of the adapted ray distribution inside the dashed ellipse in Fig. 8. As an example of how the sharper error bound is calculated, labelling ray orientations within the ellipse in Fig. 8 as grand parents (G_i), parents (P_i), and children (C_i) appropriate to their level of refinement. The error bound over the portion of adapted mesh can be written,

$$E^{G_1}_{\text{bound}} = (1-\beta)|E^{G_1}_{\text{est}}| + |E^{P_1}_{\text{est}}|, \beta = \frac{|I_{G_1} - I_{P_1}|}{\sum_{i=1}^{4} |I_{G_1} - I_{P_i}|} \tag{8}$$

where β is a correction factor. This is necessary as the error in the quadrature over the element P_1 is included twice otherwise. The form of the correction factor is prescribed by assuming the relative difference in intensity distribution is a good measure of the error distribution in the element G_1. As more levels of refinement are introduced this approximation increases in validity.

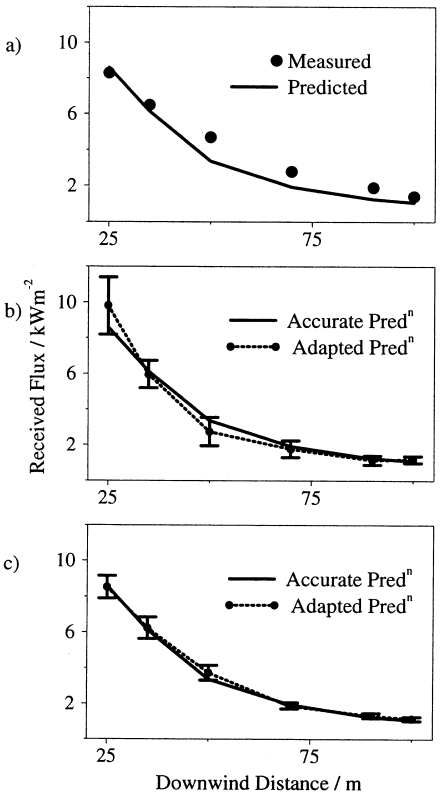

Fig. 9. Incident fluxes downstream of a sonic natural gas jet fire, (a) the ray independent prediction and measured distribution, (b) the ray independent prediction and adapted prediction with error bound (3 levels of refinement) and (c) the ray independent prediction and adapted prediction with error bound (4 levels of refinement).

Further discussion of the error bound calculated by applying (8) to the whole field of view will be continued below in relation to its application to a field scale sonic natural gas jet (pressure ratio = 1.68, diameter = 385 mm) fire. For field scale trials of natural gas flaring operations, the external radiation received by the surroundings is significant at distances up to 100 m or more downwind of the stack. Using the flame length as the most appropriate length scale, the received radiative flux is of interest up to approximately 1.5 flame lengths from the source, see Fig. 2. Taking the 1000 K temperature on the centre line as the visible flame length of the laboratory scale jet fire, the vertically orientated receivers are within 0.3 flame lengths of the jet nozzle. In this respect the laboratory scale jet fire does not give a good indication of the typical view factors encountered in modelling thermal radiation of field scale jet fires. It is likely that adaptive

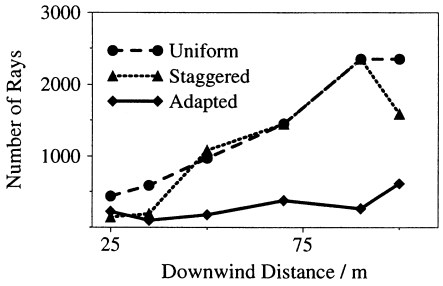

Fig. 10. Number of rays necessary to achieve a numerical error of less than 5% in the incident flux for a sonic natural gas jet fire.

quadrature should be the best quadrature strategy of those considered for this flow. To test this hypothesis a second jet fire simulation has been completed of a sonic natural gas jet fire [10].

Fig. 9(a) shows the measured incident flux for a line of receivers located downwind of the stack, 1.5 m above the ground and each orientated to nominally receive the maximum incident flux from the jet fire at their location. Also shown in the figure is a ray independent prediction of the incident flux distribution evaluated with 12,288 rays using an exponential wide-band radiation model [1]. It was estimated by additional ray refinement studies that the predicted incident flux distribution is within 0.5% of the ray converged distribution. In Fig. 9(b) and (c) predictions of incident flux and the error bound (8) with adapted ray distributions with 3 and 4 levels of refinement, respectively are shown together with the ray independent incident flux distribution. The difference between the predicted incident flux distribution and the ray independent predictions are seen to be less than the error bound. Taking the receiver locations in both jet fires discussed above and predicting the incident flux with three different levels of refinement, some 75 incident flux predictions, Eq. (8) was verified to be a true error bound. The laboratory jet fire predictions required initial ray distributions of 27 rays, $(N_\varphi,N_\theta) = (9,3)$, whereas the field scale jet fire required an initial ray distribution of 12 rays, $(N_\varphi,N_\theta) = (6,2)$ for (8) to yield an error bound in every case.

The main motivation for applying the ray effect mitigation strategies developed in this paper to a field scale natural gas jet fire was to confirm that adaptive quadrature yields significant benefits over other numerical quadrature methods for such reacting flows. In Fig. 10 the number of rays necessary to achieve a numerical error of less than 5% in the incident flux for the six receivers using a uniform, staggered and adapted ray distribution are shown. Similar to the laboratory jet fire, in the near field the staggered and adapted ray distributions are comparable, both being superior to the uniform ray distribution. In the far field the adapted ray distribution is the best strategy requiring approximately 1/7th of the number of rays required of a uniform ray distribution to achieve the same level of accuracy. The staggered ray distribution in the far field has a comparable performance to a uniform ray distribution. The reason for this ambiguous behaviour is there are two properties of the incident flux evaluation that degrade numerical efficiency, the sensitivity to perturbations in the ray distribution in the φ co-ordinate direction, and the reducing view factor with downwind distance. The staggered ray distribution mitigates the sensitivity to ray distribution in the φ co-ordinate direction but with increasing downwind distance the small view factor increases in importance.

Thus far the number of rays necessary to achieve a given numerical error has been stated to give an indication of the possible gains in efficiency of the staggered and adapted quadrature strategies over uniform quadrature. However, this is not an ideal measure for adaptive quadrature as there are additional computational overheads associated with calculating the error estimates in the adaption criteria and the data structure used to store the discrete incident intensity distribution is more complex. Comparing the run-time to achieve a given numerical error is also not a good indication of computational cost as in general the numerical error is not available and a ray refinement study is necessary to confirm ray convergence. The run-times to complete a ray refinement study for the receiver 100 m from the fire source are 563 s and 2813 s for adaptive and uniform quadrature, respectively. Using the uniform quadrature scheme, ray convergence is inferred when doubling the number of rays in each co-ordinate direction changes the predicted flux by less than 5%. Whereas for the adaptive quadrature scheme ray convergence is inferred when the error bound is less than 5%. The timing data given above was for simulations on a Silicon Graphics R4000 workstation.

5. Conclusion

Two quadrature strategies for mitigating the ray effect in jet fire radiation modelling have been described. The first quadrature strategy was to stagger the ray distribution in the φ co-ordinate direction. This relatively simple modification improves the rate of convergence and convergence behaviour generally such that Richardson extrapolation can be applied successfully to derive an error estimate. Use of the error estimate reduces the need for an expensive ray refinement study. A staggered ray distribution is an efficient quadrature strategy compared to a uniform ray distribution, as it reduces the sensitivity of the incident flux prediction to the ray distribution in the φ co-ordinate direc-

tion. However, staggered ray distributions are only a partially effective strategy for mitigating the ray effect.

For receivers remote from the jet fire where the view factor from the hot emitting region is a major influence on the convergence behaviour of the predicted incident flux staggered ray distributions are only a slight improvement over uniform ray distributions. The second quadrature strategy described, in which the ray distribution automatically adapts in response to the variation in the incident intensity distribution, was shown to be successful at reducing the computational cost of calculating the incident flux at locations remote from the jet fire. Similar to the staggered ray distribution strategy, a sharp error bound derived from the extrapolated error formula (5) suitably modified (8) for partially refined hemispherical elements reduces the need for expensive ray refinement studies.

The quadrature strategies have been demonstrated by application to two jet fires to be an improvement over the original uniform non-adaptive quadrature method used by Shah [13]. Comparing the two quadrature strategies, staggered ray distributions are simple to implement and for near field jet fire radiation modelling comparable if not superior to adaptive quadrature. The benefits of using adaptive quadrature must be weighed against the additional complexity of implementation. That said, the implementation is a once and for all activity that can be discounted over many years, for a model that is to be applied to many different reacting flows. A further consideration is the adaptive quadrature strategy can more easily be automated, reducing the risk of bogus heat transfer predictions due to poor problem specification by a user not well acquainted with thermal radiation modelling.

Although the focus has been ray effect mitigation in free jet fire simulation, the methods described could be applied successfully to other reacting flows provided a small hot volume of gas dominates the heat transfer. Similarly, although the radiation solver used is the discrete transfer method, the staggered ray quadrature strategy could be implemented in other radiation solvers such as the discrete ordinates method.

Acknowledgements

This paper is published by permission of BG Plc. A proportion of this work was funded under a CEC ESPRIT contract, Nr 8835 — TANIT.

References

[1] P.S. Cumber, M. Fairweather, S. Ledin, Application of wide band radiation models to non-homogeneous combustion systems, International Journal of Heat and Mass Transfer 41 (1998) 1573–1584.
[2] J.S. Truelove, Mixed-grey-gas model for flame radiation, AERE R 8494, UKAEA, Harwell, UK, 1976.
[3] J.C. Chai, H.S. Lee, S.V. Patankar, Ray effect and false scattering in the discrete ordinates method, Numerical Heat Transfer B 24 (1993) 373–389.
[4] F.C. Lockwood, N.G. Shah, A new radiation solution method for incorporation in general combustion prediction procedures, in: Eighteenth Symposium (Int.) on Combustion, The Combustion Institute, Pittsburgh, 1981, pp. 1405–1414.
[5] S. Baillie, M. Caulfield, D.K. Cook, P. Docherty, A phenomenological model for predicting the thermal loading to a cylindrical vessel impacted by high pressure natural gas jet fires, Trans. IChemE Part B 76 (1998) 3–13.
[6] S.M. Jeng, M.C. Lai, G.M. Faeth, Nonluminous radiation in turbulent buoyant axisymmetric flames, Combustion Science and Technology 40 (1984) 41–53.
[7] D.B. Spalding, GENMIX: A General Computer Program for Two-Dimensional Parabolic Phenomena, Pergamon Press, Oxford, 1977.
[8] W.P. Jones, B. Launder, The prediction of laminarization with a two-equation model of turbulence, International Journal of Heat and Mass Transfer 15 (1972) 301–314.
[9] M. Fairweather, W.P. Jones, R.P. Lindstedt, A.J. Marquis, The predictions of a turbulent reacting jet in a crossflow, Combustion and Flame 84 (1991) 361–375.
[10] D.K. Cook, P.S. Cumber, M. Fairweather, F. Shemirani, Modelling free and impacting underexpanded jet fires, in: Process Safety — The Future, Hazards XIII, IChemE, Manchester, UK, 1997.
[11] P.S. Cumber, Improvements to the discrete transfer method of calculating radiative heat transfer, International Journal of Heat and Mass Transfer 38 (1995) 2251–2258.
[12] C.F. Gerald, P.O. Wheatley, Applied Numerical Analysis, 3rd ed, Addison-Wesley, London, 1984.
[13] N.G. Shah, New method of computation of radiant heat transfer in combustion chambers, Ph.D. Thesis, University of London, 1979.